DOI: 10.1002/chem.201000216

Symmetrical and Nonsymmetrical Chromophores with Tröger's Base Skeleton: Chiroptical, Linear, and Quadratic Nonlinear Optical Properties—A Joint Theoretical and Experimental Study

Sergey Sergeyev,*[a, b] Delphine Didier,[b] Vitaly Boitsov,[b] Ayele Teshome,[c] Inge Asselberghs,[c] Koen Clays,[c] Christophe M. L. Vande Velde,[d] Aurélie Plaquet,[e] and Benoît Champagne[e]

Dedicated to Professor Manfred Hesse on the occasion of his 75th birthday

Abstract: We report on the novel chiral push–pull chromophores derived from 6*H*,12*H*-5,11-methanodibenzo-[*b*,*f*][1,5]diazocine (Tröger's base skeleton). The synthesis of symmetrical chromophores featuring two identical acceptors, as well as the synthesis of unsymmetrical chromophores featuring only one acceptor is given. Symmetrical chromophores were prepared in the enantiomerically pure form and their chiroptical properties were investigated. Second-order nonlinear optical (NLO) properties of new chromophores were investigated with the aid of hyper-Rayleigh scattering (HRS). The detailed theoretical analysis of the second-order NLO properties of the chromophores was also undertaken. The joint theoretical and experimental studies of chromophores derived from Tröger's base skeleton, in comparison with benchmark chromophores featuring a dimethylamino group as the donor, provided insight into the relationship between the structure of the new chromophores and their NLO properties.

Keywords: chirality · chromophores · hyper-Rayleigh scattering · nonlinear optics · Tröger's base

Introduction

Tröger's base (2,8-dimethyl-6*H*,12*H*-5,11-methanodibenzo-[*b*,*f*][1,5]diazocine **1a**, Scheme 1) is a chiral diamine with two stereogenic bridgehead nitrogen atoms. Analogues of Tröger's base are easily accessible through the condensation of the corresponding anilines with formaldehyde or its syn-

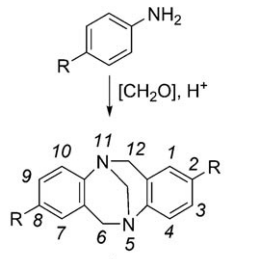

1a (= Tröger's base): R = Me
1b: R = H; **1c**: R = Br; **1d**: R = I

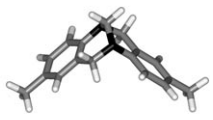

Scheme 1. Left: the synthesis of Tröger's base analogues from anilines (the numbering of 6*H*,12*H*-5,11-methanodibenzo[*b*,*f*][1,5]diazocine according to IUPAC rules is shown). Right: the optimized geometry of (*S*,*S*)-**1a**.

[a] Dr. S. Sergeyev
University of Antwerp, Department of Chemistry
Groenenborgerlaan 171, 2020 Antwerp (Belgium)
Fax: (+32) 3-2653233
E-mail: serguei.sergueev@ua.ac.be

[b] Dr. S. Sergeyev, Dr. D. D. Didier, Dr. V. Boitsov
Université Libre de Bruxelles (ULB)
Laboratoire de Chimie des Polymères
CP 206/01, Boulevard du Triomphe, 1050 Brussels (Belgium)

[c] A. Teshome, Dr. I. Asselberghs, Prof. K. Clays
Department of Chemistry, University of Leuven
Celestijnenlaan 200D, 3001 Leuven (Belgium)

[d] Dr. C. M. L. Vande Velde
Karel de Grote University College
Department of Applied Engineering
Salesianenlaan 30, 2660 Antwerp (Belgium)

[e] A. Plaquet, Prof. B. Champagne
Laboratoire de Chimie Théorique
Facultés Universitaires Notre-Dame de la Paix (FUNDP)
Rue de Bruxelles 61, 5000 Namur (Belgium)

Supporting information for this article is available on the WWW under http://dx.doi.org/10.1002/chem.201000216.

thetic equivalent. The unique set of structural features (C_2 symmetry and a rigid V-shaped geometry with the two aromatic rings nearly perpendicular to each other) makes derivatives of Tröger's base very attractive as nanometer-sized molecular scaffolds for supramolecular chemistry and molecular recognition. The chemistry of Tröger's base analogues has been extensively reviewed;[1,2] additional examples of applications not covered by these reviews can be found in further recent publications.[3] Most applications of these compounds reported to date have exploited the folded geometry and, in some instances, the chirality of Tröger's base. Another interesting structural feature, namely, the two tertiary amine functionalities, has hardly been used until now. Due to the presence of two nitrogen atoms, Tröger's base can be viewed as a structural analogue of the *N*,*N*-dialkylanilines, which have found extensive application in the design of chromophores with nonlinear optical (NLO) properties.[4] Recently, the use of Tröger's base in the design of V-shaped push–pull chromophores comprising pyridinium acceptors, which have proven to be highly efficient in linear chromophores,[5] was pioneered. Interesting solid-state fluorescence properties of these V-shaped chromophores were reported, but no information on their NLO properties was disclosed.[6]

In the course of our own study on chromophores with potential NLO activities, we decided to explore the chiral, V-shaped scaffold of 6*H*,12*H*-5,11-methanodibenzo[*b*,*f*]-[1,5]diazocine, which provides the possibility to incorporate two chromophoric units within one molecule, in addition to their dipole moments being nonantiparallel to one another. The introduction of chiral elements within the conjugated system might prove beneficial in obtaining noncentrosymmetrical crystals. The latter feature constitutes an important prerequisite for the observation of bulk second-order NLO phenomena. Examples of V-shaped push–pull chromophores are known. For instance, axially chiral C_2-symmetrical binaphthyl derivatives have exhibited high first hyperpolarizabilities.[7] Other V-shaped systems have been suggested as NLO chromophores,[8] as exemplified by various derivatives of the (dicyanomethylene)pyran[9] in which strong electronic interactions between the two chromophores occur, since they share the same acceptor group. This leads to specific relationships between the opening angle, donor/acceptor strengths, and first hyperpolarizability of these compounds. In the case of Tröger's base derivatives, these interactions are expected to be small because the two chromophores have distinct nitrogen donor atoms, though they are close to one another.

In a recent preliminary account,[10] the synthesis and theoretical studies of the racemic chromophores **2** and **3**, derived from 6*H*,12*H*-5,11-methanodibenzo[*b*,*f*][1,5]diazocine and featuring two identical acceptors, were reported. Herein, we wish to disclose the synthesis of these chromophores in enantiopure form, as well as the synthesis of the unsymmetrical chromophores **4** and **5**, which feature only one acceptor. We also report on the chiroptical properties and on the joint theoretical and experimental studies of the quadratic NLO properties of these compounds in comparison with the benchmark chromophores **6** and **7**, which feature the dimethylamino group as the donor.

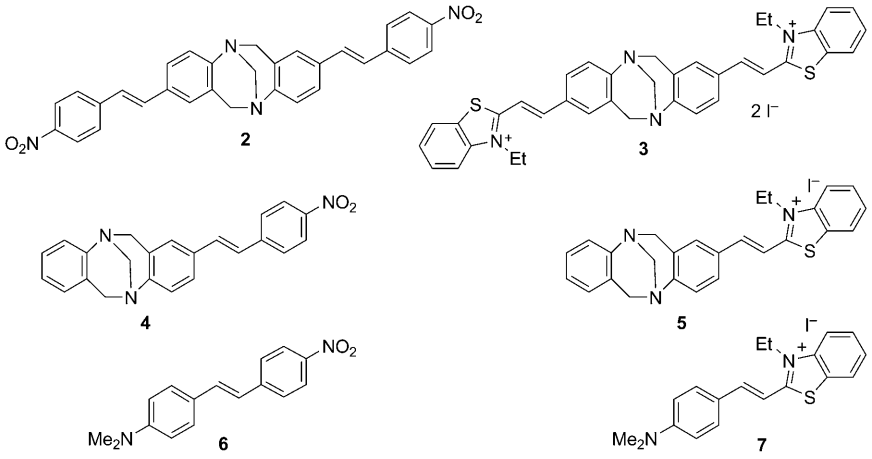

Results and Discussion

Synthesis: The synthesis of the racemic symmetrical chromophores (±)-**2** and (±)-**3** was described by us earlier (Scheme 2).[12,13] For the synthesis of the enantiomerically pure chromophores, we used the same route starting from the enantiomerically pure iodide **1d**.

Since Tröger's base and its analogues easily racemize in acidic media, chromatography on chiral stationary phases (CSP) appeared to be the method of choice for the enantioseparation of the racemate on a relatively small scale.[14–16] On an analytical scale, enantiomers of diiodide **1d** has previously been separated with very good selectivity on commer-

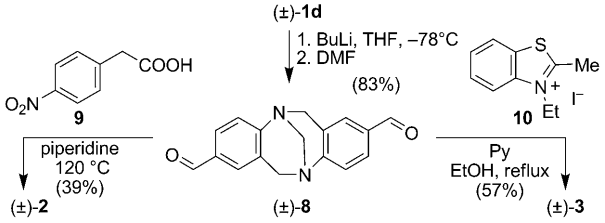

Scheme 2. The synthesis of the racemic, symmetrical chromophores (±)-**2** and (±)-**3** from (±)-**8**. For the synthesis of enantiomerically pure **2** and **3**, the same reagents and conditions were used, but starting from (*S*,*S*)-**1d** or (*R*,*R*)-**1d**.

cial CSP Whelk O1.[17] We successfully scaled up this method for semipreparative separation; complete enantioseparation of approximately 200 mg of racemic (±)-**1d** was easily achieved in a single run on a 20×250 mm column (Figure 1, see the Experimental Section for details). The

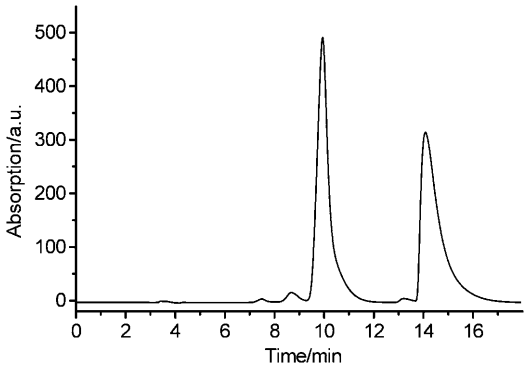

Figure 1. The semi-preparative HPLC enantioseparation of **1d** on a Whelk O1, 20×250 mm column; mobile phase hexane/*i*PrOH 95:5.

subsequent transformation of both enantiomers of **1d** into enantiomerically pure **2** and **3** was performed in basic or neutral conditions, hence no racemization occurred. This rare example of synthetic transformations on the methanodibenzo[*b*,*f*][1,5]diazocine skeleton with conservation of stereochemical integrity demonstrates the general synthetic potential of enantiomerically pure Tröger's base analogues.

For detailed insight into the NLO properties (see below), we were interested in the comparison between the symmetrical chromophores (±)-**2** and (±)-**3** and the unsymmetrical chromophores (±)-**4** and (±)-**5**. For the synthesis of (±)-**4** and (±)-**5**, a similar strategy as that for (±)-**2** and (±)-**3** was used, starting from bromide (±)-**11**. The synthesis of unsymmetrical Tröger's base analogues is less trivial than that of symmetrical ones, which are easily accessible from the corresponding anilines. Although several procedures have earlier been reported for the preparation of (±)-**11**,[12,18] the recently developed electrophilic halogenation of (±)-**1b**[19] appears most practical. Subsequently, bromide (±)-**11** was converted into aldehyde (±)-**12** and then into chromophores (±)-**4** and (±)-**5** (Scheme 3).

Chiroptical properties and absolute configuration: Initially we intended to take advantage of the presence of the heavy iodine atom in **1d** for the assignment of its absolute configuration with "anomalous X-ray scattering". Unfortunately, we did not succeed in growing suitable crystals; solvates were formed, which rapidly lost the solvent and therefore did not produce satisfactory XRD results. Hence, we decided to assign the absolute configurations of the enantiomers of **1d** by comparing the circular dichroism (CD) spectra with that of a structural analogue.

It is well known that comparing CD spectra for the assignment of absolute configuration has to be used with cau-

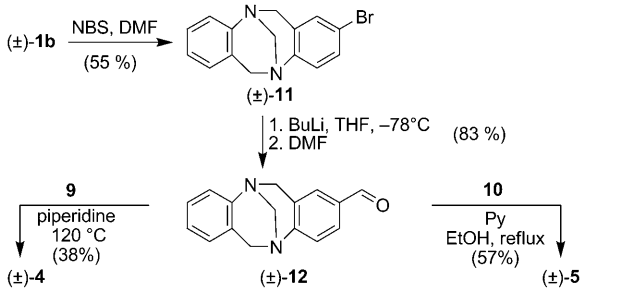

Scheme 3. The synthesis of the racemic, unsymmetrical chromophores **2** and **3** from (±)-**1b**.

tion, since the donor/acceptor nature of substituents can seriously affect the appearance of CD spectra and render such a comparison unreliable. In the particular case of Tröger's base analogues, the existence of a correlation between the sign of the lowest-energy Cotton effect and the absolute configuration was shown by Kostyanovsky and co-workers.[20] Lützen and co-workers have, however, demonstrated that this comparison can be misleading in some cases.[16] Hence, we have chosen a derivative with electronic properties as close as possible to diiodide **1d**, namely, dibromide **1c**, as a reference. Dibromide **1c** was resolved by the same method used for **1d** and crystals of sufficient quality for XRD studies were obtained. A crystal of (−)-**1c** gave a value for the Flack parameter[21] of $R=0.01(0.004)$ and its configuration was unambiguously assigned as (*R*,*R*). CD spectra of the two enantiomers of iodide **1d** are shown in Figure 2, together with the spectra of the two enantiomers

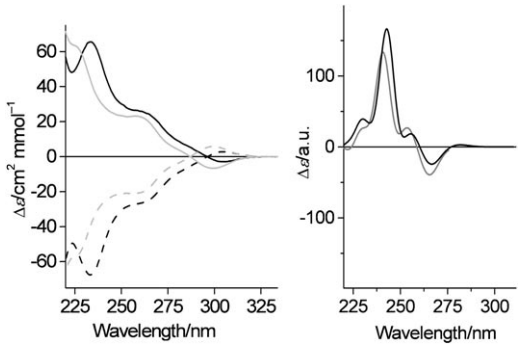

Figure 2. Left: experimental CD spectra of (+)-(*S*,*S*)-**1c** (grey solid line), (+)-(*S*,*S*)-**1d** (black solid line), (−)-(*R*,*R*)-**1c** (grey dashed line), and (−)-(*R*,*R*)-**1d** (black dashed line). Right: simulated CD spectra of (+)-(*S*,*S*)-**1c** (grey line) and (+)-(*S*,*S*)-**1d** (black line).

of dibromide **1c**. Based on the very similar shape of the CD curves, a confident assignment of the absolute configuration can be made from the sign of the longest-wave Cotton effect.[20] Since the stereochemistry of **1d** must be retained during its subsequent transformation into **2** and **3**, the assignment of the absolute configuration of the chromophores through chemical correlation becomes possible. This assignment is supported by time-dependent DFT (TDDFT) calcu-

lations of the excitation energies and rotatory strengths, which were then used to simulate the CD spectra (Figures 2 and 3).

The CD spectra of the push–pull chromophores **2** and **3** (Figure 3) are dramatically different from those of **1c,d**; they are dominated by strong, longwave Cotton effects with the maximum wavelength approximately coinciding with the maxima in their absorption spectra: $\lambda_{max,\,CD}$ (EtOH) 390 and 450 nm and $\lambda_{max,\,abs}$ (EtOH) 382 and 433 nm for **2** and **3**, respectively.[10]

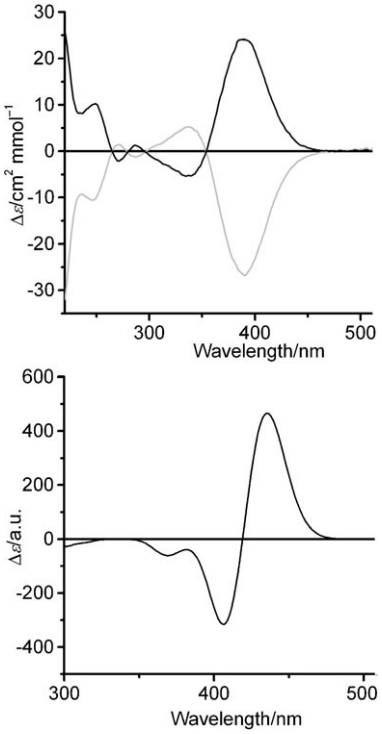

Figure 3. Top: experimental CD spectra of chromophores (*S*,*S*)-**2** (black line) and (*R*,*R*)-**2** (grey line). Bottom: simulated CD spectrum of chromophore (*S*,*S*)-**2**.

Linear and second-order NLO properties: The linear and second-order NLO properties for the chromophores used in this study are reported in Table 1. The first observation is the longer wavelength of maximal absorption ($\lambda_{max,\,abs}$) for all the benzothiazolium acceptor-based chromophores (**3**, **5**, and **7**) compared with the corresponding analogues that have the nitro group as an acceptor (**2**, **4**, and **6**). This is in agreement with other studies that compare the electron-accepting strength of the benzothiazolium moiety with that of more conventional acceptors, such as the nitro group.[22] Congruent with this observation in linear optics are the experimental results in second-order nonlinear optics.

The static first hyperpolarizability values $\beta_{HRS,0}$ (i.e., the experimentally obtained dynamic values $\beta_{HRS,800}$, corrected for different degrees of resonance enhancement) are all approximately two times larger for the benzothiazolium-derived compounds (**3**, **5**, and **7**) than for the corresponding 4-nitrophenyl analogues (**2**, **4**, and **6**). This is a confirmation of the relative acceptor strengths and is not related to the use of Tröger's base as an alternative electron-donor moiety. Note that the dynamic hyperpolarizability values $\beta_{HRS,800}$ are larger for all the chromophores based on the nitrophenyl acceptor, but this is only due to this resonance enhancement when using a fundamental laser wavelength of 800 nm, for which the second-harmonic wavelength of 400 nm is very close to the electronic resonance.

Table 1. Linear optical properties,[a] NLO properties,[b] and the derived opening angle.[c,d]

	$\lambda_{max,\,abs}$ [nm]	ε_{max} [$L\,mol^{-1}\,cm^{-1}$]	$\beta_{HRS,800}$, [10^{-30} esu]	$\beta_{HRS,0}$, [10^{-30} esu]	ρ[e]	θ [°]
2	391	50800	178±12	6.2±1	3.0±0.4	76±5
3	436	56200	107±6	14±1	2.5±0.2	77±5
4	389	24000	182±15	7.4±1	3.8±0.2	–
5	433	20500	110±10	14±1	4.2±0.3	–
6	443	30200	174±12	27±2	3.7±0.2	–
7	525	59000	120±4	49±2	3.7±0.2	–

[a] $\lambda_{max,\,abs}$ is the wavelength of maximal absorption and ε_{max} is the extinction coefficient at $\lambda_{max,\,abs}$. [b] $\beta_{HRS,800}$ is the dynamic first hyperpolarizability determined at a fundamental wavelength of 800 nm, $\beta_{HRS,0}$ is the static first hyperpolarizability derived with the two-state approximation, and ρ is the depolarization ratio. [c] The angle between two arms of Tröger's base bischromophoric derivatives (θ). [d] All Measurements taken in DMF. [e] A value of 1.5±0.1 was obtained for the octopolar reference chromophore crystal violet, in agreement with the theoretical value of 1.5.

A second observation is the blueshift of the absorption spectra upon replacing the dimethylaminophenyl donor moiety by the Tröger's base skeleton. In compounds derived from both the nitrophenyl and benzothiazolium acceptors, a substantial blueshift is observed. For the bischromophoric compounds **2** and **3** this has been observed before.[10] This experimental observation was rationalized by theoretical calculations in terms of reduced conjugation between the lone pair on the nitrogen atom and the aromatic ring in the Tröger's base skeleton, compared with *N*,*N*-dimethylaniline. This is due to the geometric constraints imposed by the bridgehead nitrogen atom in Tröger's base. Nevertheless, it has been suggested (and supported by the observation of the reactivity of methanodibenzo[*b*,*f*][1,5]diazocine ((±)-**1b**) in aromatic electrophilic substitutions) that conjugation between the lone pair of the nitrogen atom and the aromatic ring is not negligible.

The present work now shows, in addition, the impact on the second-order NLO properties of this "partial conjugation" due to geometric constraints. The static first hyperpolarizability values $\beta_{HRS,0}$ (i.e., the experimentally obtained dynamic values $\beta_{HRS,800}$, corrected for different degrees of resonance enhancement) are all substantially smaller for the Tröger's base derivatives (**2**–**5**) than for analogues with the dimethylaminophenyl donor (**6**, **7**). This is in agreement with the expectations based on the observation of the blueshifts in linear absorption spectra. Less conjugation with the

nitrogen-derived donor moiety in Tröger's base will also mean that it is a less efficient donor.

Availability of both the mono- and the bischromophoric systems allowed a more detailed comparative study towards the effectiveness of the Tröger's base molecular scaffold for nonlinear optics. It had been conjectured that the monochromophoric derivative **4** could be a good monomeric reference chromophore with respect to the bischromophoric derivative **2** based on the very small splitting calculated between the two highest occupied and the two lowest unoccupied molecular orbital energy levels.[10] In this study, the theoretical conjecture was experimentally confirmed as the electronic spectral properties for both the mono- and the bischromophoric structures (**2** vs. **4** and **3** vs. **5**) are essentially identical, whereas the oscillator strength for the bischromophoric compounds is roughly twice the value for the monochromophoric reference compounds (see Table 1). Figure 4 compares the linear optical properties (UV/Vis absorption spectra) of the nitrophenyl acceptor-based benchmark **6**, the monochromophoric compound **4**, and the bischromophoric compound **2**. These observations confirm that the electronic coupling between the two separate arms of the bischromophoric compound is small; there is rather a conservation of the original confinement of the conjugation in the two separate arms of the bischromophoric compound.

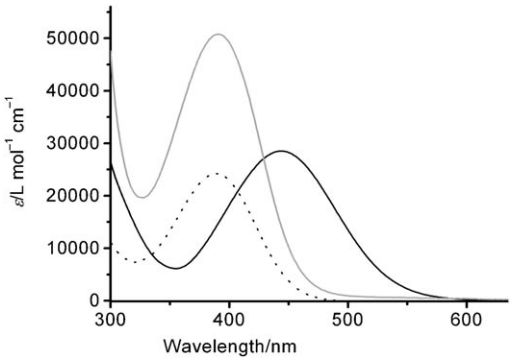

Figure 4. UV/Vis absorption spectra of **2** (grey line), **4** (black dashed line), and **6** (black solid line) in DMF.

This negligible coupling then allows for a simple structural analysis of the second-order NLO properties for both the mono- and the bischromophoric compounds in terms of the opening angle between the two chromophores.[23] If the monochromophoric compound can be used as the "monomer" model (as supported by the absorption properties, see above) for the bischromophoric compound (the "dimer"), the vector addition model results in a relationship between the first hyperpolarizability of the dimer β_{dimer} and the first hyperpolarizability of the monomer β_{mono}, and the opening angle θ between the two "monomers" can be estimated as $\beta_{zzz}(\text{dimer}) = 2\beta_{zzz}(\text{monomer})\ [\cos(\theta/2)]^3$, in which the diagonal tensor components are obtained using $\beta_{zzz} = ((35/6)^{1/2})\beta_{HRS}$.

When applying this relationship to the dynamic hyperpolarizability values, $\beta_{zzz,800}$, the values for the opening angles reported in Table 1 result. These data suggest that the opening angles between the two chromophoric moieties for Tröger's base analogues **2** and **3** would be (76 ± 5) and $(77 \pm 5)°$, respectively. From the XRD studies it is known that the angles between the planes of aromatic rings of Tröger's base analogues featuring the methanodiazocine moiety fused with various (hetero)aromatic rings typically fall within 85–105° range,[2] although "extreme" values as small as 80.2[24] or as large as 113.9°[25] have been encountered. This spread is largely due to crystal-packing effects; semi-empirical geometry optimization predicts an approximately 100° angle between the plane of the aromatic rings for 6*H*,12*H*-5,11-methanodibenzo[*b*,*f*][1,5]diazocine derivatives.[26] The values obtained from DFT geometry optimization are 103 and 108° for **2** and **3**, respectively. Since the angle between the planes of the aromatic rings and the opening angle between the dipole moment vectors of the two chromophores do not exactly coincide, the estimation obtained from the analysis of dynamic hyperpolarizability values is quite reasonable. Further limitations of the model are: 1) the assumption that the β_{HRS} value of the dimeric chromophore is dominated by β_{zzz}, which leads to an underestimation of θ because β_{zzz} is overestimated and the β_{zxx} component is underestimated and 2) the neglect of cross-polarization interactions between the chromophore units, which usually decreases the global response. Note that when the same relationship is applied to the static hyperpolarizability values, $\beta_{zzz,0}$, essentially the same values result, since the degree of resonance enhancement is also essentially identical; this is due to the similar value for $\lambda_{max,\ abs}$ for both the "monomer" and the "dimer".

Additional experiments in the form of the measurement of the depolarization ratio ρ for the nonlinear scattering confirm that the monomeric chromophores **4** and **5** are good "monomeric" model compounds. A good monomeric model compound should have a β_{zzz} along the molecular dipolar z axis. This then justifies relating the experimental result β_{HRS}, to just one tensor component by using $\beta_{zzz} = \beta_{HRS}\ (35/6)^{1/2}$. A single major hyperpolarizability tensor component β_{zzz} along the dipolar molecular z axis shows up experimentally as a relatively large depolarization ratio. In theory, for a purely dipolar contribution without any off-axis contribution, and for a depolarization measurement with infinitely small numerical aperture and with the entire signal coming from the solute chromophore, this ratio should be equal to five. For real molecules and in actual practice, this value is, however, lowered by non-zero off-diagonal contributions, by a finite aperture, and by solvent contribution to the signal. A value of 3.4 has been reported for dipolar benchmark compounds such as Disperse Red 1.[23,27] The experimental observation that the depolarization ratio is relatively large for both the Tröger's base monochromophoric analogues **4** and **5** and also for our benchmark compounds **6** and **7** indicates that the second-order NLO response of these chromophores is dominated by the single major hyperpolarizability tensor component β_{zzz}. The lower values observed for the depolari-

zation ratio of the bischromophoric compounds **2** and **3** is completely in line with our model.

Theoretical analysis of NLO data: Hyper-Rayleigh scattering (HRS) data (β_{HRS} and ρ) of compounds **2**–**7** calculated at the MP2/6-31G* level of approximation and taking into account the solvent effects within the polarizable continuum model (PCM) scheme show that the dipolar character of the compounds decreases when going from compounds **4** and **6** to **2** (or from **5** and **7** to **3**) (Table 2). This is evidenced by the depolarization ratios, which change from the almost ideal dipolar value ($\rho=5$) to 3.72 and 2.88, respectively. This is further confirmed by the approximate β_{HRS} and ρ values that can be calculated by using either only one dominant β tensor component for the dipolar molecules **4**–**7**, or two dominant β tensor components for V-shaped molecules **2** and **3**, and which closely match the full values. Thus, the β_{HRS} values of **4**–**7** are fully determined by one tensor component, whereas two are necessary to obtain the values for **2** and **3**. Note that, when using compound **2** as the example, only the $\beta_{zzz,0}$ value cannot reproduce the β_{HRS} value (12 vs. 42 for the full $\beta_{HRS,0}$ value).

Table 2. Theoretical NLO properties[a] and opening angle.[b,c]

	$\beta_{zzz,0}$, [10^{-30} esu]	$\beta_{xxz,0}$, [10^{-30} esu]	$\beta_{HRS,0}$, [10^{-30} esu][d]	ρ[e]	$\beta_{HRS,0}$, (full), [10^{-30} esu]	ρ (full)	θ [°]
2	30	60	41	3.73	42	3.72	100
3	30	97	64	3.18	63	2.88	104
4	76	–	31	5.00	33	4.90	–
5	162	–	67	5.00	68	4.75	–
6	171	–	71	5.00	71	4.89	–
7	336	–	139	5.00	138	4.96	–

[a] $\beta_{zzz,0}$ and $\beta_{xxz,0}$ are the dominant components of the static first hyperpolarizability tensor, $\beta_{HRS,0}$ is the HRS first hyperpolarizability, and ρ is the depolarization ratio for nonlinear scattering calculated at the IEFPCM/MP2/6-31G* level of approximation. [b] Angle between the two arms of Tröger's base derivatives (θ) determined from B3LYP/6-311G* geometry optimizations. [c] The full $\beta_{HRS,0}$ and ρ values (columns 6 and 7) are also given as well as approximates (columns 4 and 5), calculated from only one or two dominant tensor components to address the dimensionality of the NLO-phore. [d] For the V-shaped molecules **2** and **3** $\beta_{HRS,0}=\beta_{zzz,0}\ [(18+16R+38R^2)/105]^{1/2}$; for the linear molecules **4**–**7**, $\beta_{HRS,0}=\beta_{zzz,0}\ [(6/35]^{1/2}$. [e] For the V-shaped molecules $\rho=(15+18R+27R^2)/(3-2R+11R^2)$, with $R=\beta_{xxz,0}/\beta_{zzz,0}$; for the linear molecules $\rho=5$.

It is comforting to observe that these theoretical predictions for the depolarization ratio are in good agreement with the experimental observations, taking into account the above-mentioned practical considerations. For the monochromophoric Tröger's base derivatives **4** and **5** and for the benchmark chromophores **6** and **7**, the calculated values are identical to or almost equal to the limiting value of five, but for the V-shaped bischromophoric "dimers" **2** and **3**, these values are substantially lower. Within these two lower values, we can further differentiate between the nitro-acceptor-based compound **2** (intermediate value) and the benzothiazolium acceptor-based compound **3** (the lowest value for the calculated depolarization ratio). The observation that the experimental values for these depolarization ratios also reflect this differentiation beyond the estimated statistical uncertainty, strengthens our assumption for the analysis of the solution-phase structure of the bischromophoric Tröger's bases **2** and **3**.

To further compare the experimental and theoretical β values, a pre-treatment of the experimental data was necessary. Indeed, the experimental data are impacted by resonance conditions since the measurements are carried out at a frequency within the absorption band, slightly above or below the maximum, whereas this effect is absent in the calculations. Evaluating the magnitude of this effect is, however, difficult.[28] The simplest way to estimate the impact of frequency dispersion in pseudo-dipolar chromophores is to consider the two-state approximation,[29] which assumes that only one excited state contributes to the second-order NLO response. Considering a homogeneous damping γ and neglecting the nonresonant terms,[30] the frequency-dispersion factor for any of the diagonal components of the first hyperpolarizability tensor $F(\omega,\omega_{ge},\gamma)$ is as shown in Equation (1):

$$F(\omega,\omega_{ge},\gamma)=\frac{\beta_{zzz}(-2\omega;\omega,\omega)}{\beta_{zzz}(0;0,0)}=\frac{\omega_{ge}^2(\omega_{ge}-i\gamma)^2}{\left([\omega_{ge}-i\gamma]^2-4\omega^2\right)\left([\omega_{ge}-i\gamma]^2-\omega^2\right)} \quad (1)$$

in which g and e are the two electronic, ground and excited, states contributing to the β value, and ω_{ge} is the corresponding excitation energy. Assuming that the same treatment can be applied to the off-diagonal β_{zxx} component, which is a good approximation because the splitting of the excitation energies is small, the extrapolated static β values obtained by setting γ to zero as well as by choosing γ values matching the half width at half maximum (HWHM) of the corresponding absorption spectra (i.e., $\gamma\approx1.2$ HWHM of the $e^{-[(\omega-\omega_{ge})/\gamma]^2}$ Gaussian function) are shown in Table 3. These estimates of the dispersion factors have then been improved by incorporating an inhomogeneous broadening based on the absorption spectrum, which implicitly contains information on the distribution of the transition frequencies as well as taking into account the vibronic structure of the excited

Table 3. Comparison between extrapolated and calculated first hyperpolarizabilities values $\beta_{HRS,0}$.[a]

	Extrapolated from Equation (1), $\gamma=0$	Extrapolated from Equation (1), $\gamma\neq0$	Extrapolated from Equations (2) and (3)	Calculated (MP2/IEFPCM)
2	6.2	40	11	42
3	14	29	9.1	63
4	7.4	34	10	33
5	14	29	9.1	68
6	27	51	16	71
7	49	55	39	138

[a] All values are given in 10^{-30} esu.

states. According to Campo et al.,[28] for an incoherent process such as HRS, the dispersion factor reads as for Equation (2):

$$\left|\frac{\beta^{HRS}(-2\omega;\omega,\omega)}{\beta^{HRS}(0;0,0)}\right| = \left\{\int N\left(\omega'_{ge}\right)\left|F\left(\omega,\omega'_{ge},\gamma\right)\right|^2 d\omega'_{ge}\right\}^{1/2} \tag{2}$$

in which the $N(\omega'_{ge})$ value, the normalized distribution of the transition frequencies, is approximated by a Gaussian function reproducing the experimental HWHM of the corresponding main absorption band. Moreover, the distribution of the transition frequencies can further be improved by considering the single-mode vibronic model and replacing $N(\omega'_{ge})$, as shown in Equation (3):

$$N\left(\omega'_{ge}\right) = \sum_{n}^{\text{vib. levels}} \left[\frac{S^n e^{-S}}{n!}\right] e^{-\left[\left(\omega'_{ge}-\omega_n\right)/\gamma_{vib}\right]^2} \tag{3}$$

in which $\omega_n = \omega_{ge} + n\omega_{vib}$ corresponds to the transition from the ground state to the n^{th} vibrational level of the excited state. The Huang–Rhys factors (S) were chosen to reproduce the shape of the absorption band. The ω_{vib} and γ_{vib} values were also chosen to best reproduce the absorption spectra. This corresponds to the same approach as the one adopted in our recent work.[31] The parameters for compounds **2–7** are listed in Table 4; the corresponding simulated absorption spectra are given in the Supporting Information and show a very good correlation with experimentally obtained data. The differences between the experimental and theoretical excitation energies (e.g., 390 and 438 nm, respectively, for **2**) are typical of these TDDFT methods, also considering the fact that no vibronic structure is considered in the theoretical simulations.

Table 4. Parameters best fitting the UV/Vis absorption spectra.

	$\hbar\omega_{ge}$ [eV]; λ_{eg} [nm]	$\gamma_{homogeneous}$ [eV]	$\gamma_{inhomogeneous}$ [cm^{-1}]	S	ω_{vib} [cm^{-1}]	γ_{vib} [cm^{-1}]
2	3.17; 391	0.458	480	0.0	–	–
3	2.84; 436	0.418	480	0.5	1600	1600
4	3.19; 389	0.375	480	0.0	–	–
5	2.86; 433	0.427	480	0.5	1600	1600
6	2.80; 443	0.444	480	0.0	–	–
7	2.36; 525	0.266	480	0.5	1600	1600

Good qualitative agreement for chromophores **2–7** is obtained between theory and experiment. Therefore, by employing the values extrapolated by using Equation (1) ($\gamma = 0$), the change from one chromophore branch to two in the Tröger's base derivatives almost does not change the first hyperpolarizabilities. The β value then increases by a factor of 3–4 when going from chromophore **4** to **6** or from chromophore **5** to **7** as a result of the planarity of the nitrogen and therefore of better conjugation. These relationships are confirmed when using the other extrapolated data, although the increase of the β value due to planarity is somehow reduced. Together with the calculated MP2 values, the extrapolated data obtained from Equation (1) ($\gamma = 0$) also demonstrate the stronger acceptor character of the benzothiazolium units and the associated larger β values. The relative magnitude of the static β values is, however, not reproduced when using Equation (1) ($\gamma \neq 0$), whereas by using Equations (2) and (3), the relative magnitude is only reproduced for **6** versus **7**. These differences should be associated with the limitation of the models of extrapolation.

Conclusion

We have investigated the NLO properties of novel chiral push–pull chromophores derived from the V-shaped skeleton of 6*H*,12*H*-5,11-methanodibenzo[*b*,*f*][1,5]diazocine, a parent heterocyclic system of Tröger's base. Detailed analysis of the data led to the conclusion that molecules possessing one or two chromophoric "arms" show approximately equal HRS second-order NLO properties. This observation is very useful for future studies, since the structure of future chromophores can be chosen to be C_2 symmetric or asymmetric, based on considerations such as solubility and synthetic feasibility, without compromising their NLO properties. Between the two families of molecules studied, the systems featuring a cationic benzothiazolium acceptor have proven to be the most efficient. It was, however, demonstrated that the molecular first hyperpolarizabilities of the two families of chromophores are three to four times lower than those of analogues with a "classical" dimethylamino donor group. Notwithstanding, 6*H*,12*H*-5,11-methanodibenzo[*b*,*f*][1,5]diazocine holds considerable promise as a scaffold for NLO chromophores. Chromophores with a chiral element constituting a part of the conjugated system appear to be promising for materials with bulk NLO activity, since the introduction of chirality is an effective approach towards bulk noncentrosymmetric crystals. Such crystals have a higher number density than amorphous thin films or chromophores dispersed in a polymer matrix, a common approach that requires additional poling to orient the chromophores. Furthermore, the lower depolarization ratio and large off-diagonal tensor component for the bis-chromophoric V-shaped derivatives will translate into a lower polarization sensitivity for NLO applications.[32] Lower molecular hyperpolarizabilities can be increased by the extension of the π system and/or the incorporation of "auxiliary donors", for example, electron-rich heterocycles such as thiophene. The efficiency of this general approach was demonstrated by many previous examples.[33] We have also recently shown the efficiency of a particular combination consisting of a benzothiazolium acceptor and thiophene auxiliary donor.[34]

Experimental Section

General: All chemicals were purchased from Aldrich, Acros, or TCI Europe and used without further purification unless stated otherwise. *N*-Bromosuccinimide (NBS) was crystallized from water before use. THF was dried over benzophenone ketyl under Ar until a blue or violet color persisted. Column chromatography: SiO_2 Kieselgel 60 (Macherey–Nagel, particle size 0.04–0.063 mm). TLC: precoated SiO_2 plates Kieselgel $60F_{254}$ (Merck). Electron impact mass spectra (EIMS) were recorded on a Waters AutoSpec 6F instrument and electrospray ionization mass spectra (ESIMS) on a Waters QToF 2 instrument; *m/z* with the lowest isotopic mass are reported. ^{1}H (300 MHz) and ^{13}C NMR (75 MHz) spectra were recorded on a Brucker Avance 300 spectrometer: chemical shifts (δ) are given in ppm relative to Me_4Si (internal standard). The following derivatives were synthesized according to previously published procedures: (±)-**1b–d**,[17] (±)-**2**,[10] (±)-**3**,[10] **6**,[35] **7**,[10] (±)-**8**,[13] (±)-**11**,[19] and (±)-**12**.[12] Enantiomerically pure (*S,S*)-**8**, (*S,S*)-**2**, and (*S,S*)-**3** were prepared from (*S,S*)-**1d**, and (*R,R*)-**8**, (*R,R*)-**2**, and (*R,R*)-**3** from (*R,R*)-**1d** analogous to published procedures for the corresponding racemic compounds; NMR and MS data in all cases were essentially identical to those of the corresponding racemates. The analytical data obtained for (*S,S*)-**8** and (*R,R*)-**8** were identical to that previously published.[15] Data for enantiomers of **2**: (*S,S*)-**2**: $[\alpha]_D = 1350$ ($c = 0.01$ in CH_2Cl_2); m.p. = 237–238 °C; (*R,R*)-**2**: $[\alpha]_D = -1440$ ($c = 0.13$ in CH_2Cl_2); m.p. = 237–238 °C. Data for enantiomers of **3**: (*S,S*)-**3**: $[\alpha]_D = 1930$ ($c = 0.04$ in MeOH); m.p. = 174–175 °C; (*R,R*)-**3**: $[\alpha]_D = -2050$ ($c = 0.057$ in MeOH); m.p. = 174–175 °C.

The HPLC separations of the enantiomers of **1c,d** were performed at ambient temperature on an Agilent 1100 instrument equipped with the Rheodyne 7725 manual loop injector. Solvents were of HPLC grade. The column, (*R,R*)-Whelk-O1 (250 × 20 mm), was purchased from Regis Technologies (USA). Injection: 0.5–1.0 mL of analyte solution in CH_2Cl_2, approximately 200 mg mL^{-1}; mobile phase: hexane/*i*PrOH 95:5 (v/v), nominal flow rate 20 mL min^{-1}; detection: UV at fixed wavelength 254 nm. Separation parameters were calculated as follows: $k_1 = (t_1 - t_0)/t_0$, $k_2 = (t_2 - t_0)/t_0$, $\alpha = k_2/k_1$, $R_s = 2(t_2 - t_1)/(w_2 + w_1)$, in which t_1 and t_2 are the retention times of the first and the second eluted enantiomers, $t_0 = 3.40$ min is the void time (retention time of 1,3,5-tri-*tert*-butylbenzene), k_1 and k_2 are the retention factors of the two enantiomers, α is the separation factor, w_1 and w_2 are the widths of peaks at the base line, and R_s is the resolution at the base line. Separation parameters for **1c**: $t_1 = 8.94$ min, $t_2 = 12.27$ min, $k_1 = 1.63$, $k_2 = 2.61$, $\alpha = 1.60$, $R_s = 3.4$. Separation parameters for **1d**: $t_1 = 9.90$ min, $t_2 = 14.08$ min, $k_1 = 1.91$, $k_2 = 3.13$, $\alpha = 1.64$, $R_s = 3.3$. Data for enantiomers of **1c**, in the order of elution: (+)-(*S,S*)-**1c**: $[\alpha]_D = 393$ ($c = 0.19$ in CH_2Cl_2); m.p. = 160–162 °C; (−)-(*R,R*)-**1c**: $[\alpha]_D = -394$ ($c = 0.27$ in CH_2Cl_2); m.p. = 160–162 °C. Data for enantiomers of **1d**, in the order of elution: (+)-(*S,S*)-**1d**: $[\alpha]_D = 445$ ($c = 0.32$ in CH_2Cl_2); m.p. = 198–200 °C; (−)-(*R,R*)-**1d**: $[\alpha]_D = -454$ ($c = 0.32$ in CH_2Cl_2); m.p. = 198–200 °C.

(±)-2-[(*E*)-2-(4-Nitrophenyl)ethenyl]-6*H*,12*H*-5,11-methanodibenzo[*b*,*f*][1,5]diazocine ((±)-4): A mixture of aldehyde (±)-**12** (0.220 g, 0.879 mmol), 4-nitrobenzeneacetic acid **9** (0.479 g, 2,64 mmol), and piperidine (0.361 mL, 3.65 mmol) was heated for 20 h at 120 °C (bath temperature). The resulting mixture was cooled to RT, dissolved in CH_2Cl_2, and purified by column chromatography (SiO_2, CH_2Cl_2/AcOEt 10:1) to afford pure (±)-**4** (123 mg, 38 %). The analytically pure product was obtained by crystallization from EtOH as a crystalline yellow solid. M.p. 166–168 °C; ^{1}H NMR(300 MHz, $CDCl_3$, 25 °C): $\delta = 4.20$ (d, $^2J(H,H) = 16.5$ Hz, 1H), 4.22 (d, $^2J(H,H) = 16.5$ Hz, 1H), 4.34 (s, 2H), 4.73 (d, $^2J(H,H) = 16.5$ Hz, 2H), 6.88–7.04 (m, 3H), 7.04–7.20 (m, 5H), 7.38 (dd, $^3J(H,H) = 8.3$, $^4J(H,H) = 1.8$ Hz, 1H), 7.56 (d, $^3J(H,H) = 8.9$ Hz, 2H), 8.18 ppm (d, $^3J(H,H) = 8.9$ Hz, 2H); ^{13}C NMR (75 MHz, $CDCl_3$, 25 °C): $\delta = 58.7$, 66.9, 124.11, 124.14, 125.1, 125.2, 125.5, 125.8, 126.0, 126.6, 127.0, 127.5, 127.8, 128.3, 132.0, 132.8, 144.0, 146.6, 147.8, 149.1; HRMS (EI): *m/z*: calcd for $C_{23}H_{19}N_3O_2$: 369.1477 $[M]^+$; found: 369.1470.

(±)-(*E*)-3-Ethyl-2-[2-(6*H*,12*H*-5,11-methanodibenzo[*b*,*f*][1,5]diazocin-2-yl)ethenyl]benzothiazol-3-ium iodide ((±)-5): A mixture of aldehyde (±)-**12** (0.170 g, 0.679 mmol), 3-ethyl-2-methylbenzothiazol-3-ium iodide **10** (0.190 g, 0.622 mmol), pyridine (0.080 mL), and EtOH (8 mL) was heated at reflux for 18 h. The mixture was cooled to RT before hexane was added and the resulting solid was filtered. Crystallization from EtOH afforded pure (±)-**5** as a crystalline red solid (0.191 g, 57 %). M.p. 178–180 °C; ^{1}H NMR (300 MHz, $(CD_3)_2SO$, 25 °C): $\delta = 1.44$ (t, $^3J(H,H) = 7.5$ Hz, 3H), 4.21 (d, $^2J(H,H) = 16.8$ Hz, 1H), 4.26 (d, $^2J(H,H) = 16.2$ Hz, 1H), 4.31 (s, 2H), 4.72 (d, $^2J(H,H) = 16.8$ Hz, 1H), 4.74 (d, $^2J(H,H) = 16.2$ Hz, 1H), 4.92 (q, $^3J(H,H) = 7.5$ Hz, 2H), 6.94–7.00 (m, 2H), 7.12–7.20 (m, 2H), 7.31 (d, $^3J(H,H) = 8.4$ Hz, 1H), 7.71–7.92 (m, 5H), 8.11 (d, $^3J(H,H) = 15.6$ Hz, 1H), 8.26 (d, $^3J(H,H) = 9.3$ Hz, 1H), 8.40 ppm (d, $^3J(H,H) = 9.0$ Hz, 1H); ^{13}C NMR (75 MHz,$(CD_3)_2SO$, 25 °C): $\delta = 14.7$, 45.0, 58.6, 66.6, 112.1, 117.1, 124.2, 124.9, 125.3, 125.9, 127.5, 127.8, 128.6, 128.7, 128.9, 129.48, 129.52, 129.6, 129.7, 130.0, 141.5, 148.1, 149.6, 153.6, 172.1 ppm; HRMS (ESI): *m/z*: calcd for $C_{26}H_{24}N_3S$: 410.1961 $[M-I]^+$; found: 410.1703.

Single crystal X-ray structure determination of (−)-(*R,R*)-1c: Crystals suitable for analysis were obtained by slow evaporation of a solution in CH_2Cl_2, crystal dimensions $0.52 \times 0.43 \times 0.25$ mm; triclinic; space group *P*1; $a = 9.9052(8)$, $b = 10.2322(8)$, $c = 15.8064(12)$ Å; $\alpha = 73.6190(10)$, $\beta = 83.5210(10)$, $\gamma = 62.4250(10)$°; $V = 1362.09(18)$ Å^3; $Z = 4$; $\rho = 1852$ kg m^{-3}; $\theta_{max} = 30.09$°; graphite-monochromated $Mo_{K\alpha}$-radiation (0.71073 Å); ω-scans; $T = 140$ K; 15723 measured reflections; 13936 unique reflections; 12719 reflections $> 2\sigma(I)$; data reduction with SAINT (Bruker, 2008); multiscan absorption correction (SADABS 2008/1, Bruker, 2008); T_{min} 0.458; T_{max} 0.746; $\mu = 5.94$ mm^{-1}; structure solution and refinement SHELX97 suite of programs (Sheldrick, 2008); 685 parameters; 3 (origin fixing) restraints, hydrogen atoms placed in calculated positions and refined as riding; $R = 0.0255$ ($I > 2\sigma$(I)), $wR = 0.0589$ (all reflections); refinement against R^2; $\Delta\rho_{min} = -0.50$ e Å^{-3}, $\Delta\rho_{max} = 0.87$ e Å^{-3}; Flack parameter 0.011(4). CCDC-762694 contains the supplementary crystallographic data for this paper. These data can be obtained free of charge from The Cambridge Crystallographic Data Centre via www.ccdc.cam.ac.uk/data_request/cif.

Optical and chiroptical experiments: UV/Vis absorption spectra were measured on a Perkin–Elmer Lambda 900 spectrometer in a 1 cm cell at ambient temperature. Circular dichroism (CD) spectra were measured on a Jasco J810 spectropolarimeter. Specific optical rotations were measured on a Perkin–Elmer 141 polarimeter in a 10 cm cell at ambient temperature. Values of specific optical rotation $[\alpha]_D$ are given in 10^{-1} cm^2 g^{-1}; the concentrations *c* are in g dL^{-1}. All NLO experiments were performed at room temperature in DMF as the solvent. First hyperpolarizabilities were determined on a femtosecond hyper-Rayleigh scattering setup with a fundamental wavelength of 800 nm, with crystal violet in methanol ($\beta_{xxx,800} = 338 \times 10^{-30}$ esu) as the octopolar reference molecule. The octopolar symmetry of the reference compound was taken into account by proper weighing of its tensor component contribution to the HRS signal. The difference in solvent (methanol for the reference, DMF for the unknowns) was taken into account by solvent correction factors for the optical frequency field. The setup and the procedure have been published in more detail previously.[36] The correction for the different degrees of resonance enhancement are based on the two-state approximation and are only dependent on the closeness of the fundamental and second-harmonic wavelength to the electronic resonance wavelength ($\lambda_{max,\,abs}$).[29]

Computational details: The geometries of the Tröger's base derivatives were optimized at the DFT level using the B3LYP exchange-correlation functional and the 6-311G* basis set. The calculated optimized geometry structures are provided in the Supporting Information.

The time-dependent Hartree–Fock (TDHF)[37] and the coupled-perturbed Hartree–Fock (CPHF) schemes were employed for obtaining dynamic ($\lambda = 1064$ nm) and static first hyperpolarizabilities, respectively. These methods consist of expanding the matrices of the TDHF/CPHF equations in Taylor series of the external (static or dynamic) electric field and in solving these analytically order by order. Taking advantage of the $2n+1$ rule, only the first-order derivatives of the LCAO coefficients are needed to evaluate the β value. Solvent effects were included by using the polarizable continuum model within the integral equation formalism (IEFPCM),[38] by taking $\varepsilon_0 = 36.640$ ($\varepsilon_\infty = 1.806$) for acetonitrile. The solute cavities were built using atomic radii from the UFF force field by putting individual spheres around each heavy and hydrogen atom. To ac-

count for correlation effects, the second-order Møller–Plesset (MP2) method was employed in combination with a finite field (FF) procedure,[39] implying a Romberg Scheme to attain an accuracy on the numerical derivatives of about 1.0 a.u. (8.641×10^{-33} esu = 1 a.u. of $\beta = 3.62\times10^{-42}\ m^4V^{-1} = 3.2063\times10^{-53}\ C^3m^3J^{-2}$).[40] In many cases, the MP2 method recovers the largest part of the electron correlation effects, as estimated from higher-order methods.[41] To account for frequency dispersion at the MP2 level, the multiplicative correction scheme was applied.[42] It consists of multiplying the static MP2 value by the TDHF/CPHF ratio as shown in Equation (4):

$$\beta_{MP2}(-2\omega;\omega,\omega) \approx \beta_{MP2}(0;0,0) \times \frac{\beta_{TDHF}(-2\omega;\omega,\omega)}{\beta_{CPHF}(0;0,0)} \quad (4)$$

Moreover, the solvent effects on the first hyperpolarizabilities are determined by inserting the $\beta_{\mathrm{TDHF}}(-2\omega;\omega,\omega)$ or $\beta_{\mathrm{MP2}}(0;0,0)$ quantities evaluated within the IEFPCM scheme into Equation (4). The reported quantities are related to the HRS experiments with plane-polarized incident light and observation made perpendicular to the propagation plane. The full intensity then reads as shown in Equation (5):

$$\beta_{HRS}(-2\omega;\omega,\omega) = \sqrt{\{\langle\beta^2_{ZZZ}\rangle + \langle\beta^2_{ZXX}\rangle\}} \quad \rho = \frac{I^{2\omega}_{VV}}{I^{2\omega}_{HV}} = \frac{\langle\beta^2_{ZZZ}\rangle}{\langle\beta^2_{ZXX}\rangle} \quad (5)$$

in which $\langle\beta^2_{ZZZ}\rangle$ and $\langle\beta^2_{ZXX}\rangle$ correspond to orientational averages of the β tensor values and are calculated without assuming Kleinman's conditions (full expressions of these terms can be found in ref. [43]). The ρ value gives information on the geometry of the part of the molecule responsible for the NLO response, sometimes referred to as the NLOphore. All reported β values are given in 10^{-30} esu within the B convention. Additional hyperpolarizability values are provided in the Supporting Information.

TDDFT calculations were carried out to determine the vertical excitation energies [$\Delta E_{ge} = \hbar\omega_{ge} = \hbar(\omega_e - \omega_g)$] and the rotatory strengths necessary to simulate the CD spectra. Following a recent investigation,[44] a modified B3LYP exchange-correlation functional containing 35% of HF exchange was employed. In the case of related π-conjugated systems with donor and acceptor groups, this TDDFT approach has been found to provide excited-state properties in, at least, a good qualitative agreement with respect to experimental data.[45] Solvent effects were accounted for by using the IEFPCM scheme and the 6-311+G* basis set was employed.

The calculations were performed by using Gaussian 03[46] as well as with homemade codes to apply the Romberg differentiation scheme and to estimate the static β values from the HRS responses measured at 800 nm.

Acknowledgements

S.S. is indebted to Prof. Y. Geerts (ULB) for the opportunity to conduct an independent research program in his laboratory. This study was supported by FNRS (grant 1.5.110.08 and contract of "Collaborateur scientifique" for S.S.), by the Belgian Government (IUAP N° P06-27 "Functional Supramolecular Systems"), and by the Brussels-Capital Region ("Brains (Back) to Brussels" program). I.A. acknowledges FWO-V for a postdoctoral fellowship. A.P. is grateful to the F.R.I.A. for financial support. The calculations have been performed on the Interuniversity Scientific Computing Facility (ISCF) installed at the FUNDP, for which the authors gratefully acknowledge the financial support of the F.R.S.-FRFC and of the "Loterie Nationale" under contract no. 2.4.617.07.F, and of the FUNDP. We thank A. Remacle (ULB) and E. Franz (University of Leuven) for assistance with HPLC and CD experiments, and Prof. M. Zeller (Youngstown State University, USA) for the collection of the X-ray dataset.

[1] S. Sergeyev, *Helv. Chim. Acta* **2009**, *92*, 415; M. Valík, R. M. Strongin, V. Král, *Supramol. Chem.* **2005**, *17*, 347.
[2] B. Dolenský, J. Elguero, V. Král, C. Pardo, M. Valík, *Adv. Heterocycl. Chem.* **2007**, *93*, 1.
[3] F. R. Fischer, P. A. Wood, F. H. Allen, F. Diederich, *Proc. Natl. Acad. Sci. USA* **2008**, *105*, 17290; Y.-M. Jeon, G. S. Armatas, D. Kim, M. G. Kanatzidis, C. A. Mirkin, *Small* **2009**, *5*, 46; P. R. Brotherhood, I. J. Luck, M. J. Crossley, *Magn. Reson. Chem.* **2009**, *47*, 257; C. Michon, M.-H. Goncalves-Farbos, J. Lacour, *Chirality* **2009**, *21*, 809; E. B. Veale, D. O. Frimannsson, M. Lawler, T. Gunnlaugsson, *Org. Lett.* **2009**, *11*, 4040.
[4] S. R. Marder, *Chem. Commun.* **2006**, 131.
[5] B. J. Coe, D. Beljonne, H. Vogel, J. Garin, J. Orduna, *J. Phys. Chem. A* **2005**, *109*, 10052; C. Lambert, W. Gaschler, G. Noll, M. Weber, E. Schmalzlin, C. Brauchle, K. Meerholz, *J. Chem. Soc. Perkin Trans. 2* **2001**, 964.
[6] C.-X. Yuan, X.-T. Tao, L. Wang, J.-X. Yang, M.-H. Jiang, *J. Phys. Chem. C* **2009**, *113*, 6809; C.-X. Yuan, X.-T. Tao, Y. Ren, Y. Li, J.-X. Yang, W.-T. Yu, L. Wang, M.-H. Jiang, *J. Phys. Chem. C* **2007**, *111*, 12811.
[7] H.-J. Deussen, C. Boutton, N. Thorup, T. Geisler, E. Hendrickx, K. Bechgaard, A. Persoons, T. Bjornholm, *Chem. Eur. J.* **1998**, *4*, 240; S. V. Elshocht, T. Verbiest, M. Kauranen, L. Ma, H. Cheng, K. Y. Musick, L. Pu, A. Persoons, *Chem. Phys. Lett.* **1999**, *309*, 315; E. Hendrickx, C. Boutton, K. Clays, A. Persoons, S. van Es, T. Biemans, B. Meijer, *Chem. Phys. Lett.* **1997**, *270*, 241.
[8] M. Yang, B. Champagne, *J. Phys. Chem. A* **2003**, *107*, 3942; V. Ostroverkhov, R. G. Petschek, K. D. Singer, R. J. Twieg, *Chem. Phys. Lett.* **2001**, *340*, 109.
[9] C. R. Moylan, S. Ermer, S. M. Lovejoy, I. H. McComb, D. S. Leung, R. Wortmann, P. Krdmer, R. J. Twieg, *J. Am. Chem. Soc.* **1996**, *118*, 12950.
[10] V. Lemaur, J. Cornil, D. Didier, A. Mujawase, S. Sergeyev, *Helv. Chim. Acta* **2007**, *90*, 2087.
[11] J. Jensen, K. Wärnmark, *Synthesis* **2001**, 1873.
[12] J. Jensen, J. Tejler, K. Wärnmark, *J. Org. Chem.* **2002**, *67*, 6008.
[13] S. Sergeyev, M. Schär, P. Seiler, O. Lukoyanova, L. Echegoyen, F. Diederich, *Chem. Eur. J.* **2005**, *11*, 2284.
[14] P. R. Allen, J. N. H. Reek, A. C. Try, M. J. Crossley, *Tetrahedron: Asymmetry* **1997**, *8*, 1161; Y. Kubo, T. Ohno, J.-i. Yamanaka, S. Tokita, T. Iida, Y. Ishimaru, *J. Am. Chem. Soc.* **2001**, *123*, 12700; S. Sergeyev, F. Diederich, *Angew. Chem.* **2004**, *116*, 1770; *Angew. Chem. Int. Ed.* **2004**, *43*, 1738; S. Sergeyev, S. Stas, A. Remacle, C. M. L. Vande Velde, B. Dolensky, M. Havlik, V. Kral, J. Cejka, *Tetrahedron: Asymmetry* **2009**, *20*, 1918.
[15] S. Sergeyev, F. Diederich, *Chirality* **2006**, *18*, 707.
[16] U. Kiehne, T. Bruhn, G. Schnakenburg, R. Fröhlich, G. Bringmann, A. Lützen, *Chem. Eur. J.* **2008**, *14*, 4246.
[17] D. Didier, B. Tylleman, N. Lambert, C. M. L. Vande Velde, F. Blockhuys, A. Collas, S. Sergeyev, *Tetrahedron* **2008**, *64*, 6252.
[18] M. Faroughi, K.-X. Zhu, P. Jensen, D. C. Craig, A. C. Try, *Eur. J. Org. Chem.* **2009**, 4266.
[19] D. Didier, S. Sergeyev, *Eur. J. Org. Chem.* **2007**, 3905.
[20] D. A. Lenev, K. A. Lyssenko, D. G. Golovanov, O. R. Malyshev, P. A. Levkin, R. G. Kostyanovsky, *Tetrahedron Lett.* **2006**, *47*, 319.
[21] H. D. Flack, G. Bernardinelli, *Chirality* **2008**, *20*, 681.
[22] B. J. Coe, J. A. Harris, J. J. Hall, B. S. Brunschwig, S.-T. Hung, W. Libaers, K. Clays, S. J. Coles, P. N. Horton, M. E. Light, M. B. Hursthouse, J. Garin, J. Orduna, *Chem. Mater.* **2006**, *18*, 5907.
[23] G. Hennrich, M. T. Murillo, P. Prados, H. Al-Saraierh, A. El-Dali, D. W. Thompson, J. Collins, P. E. Georghiou, A. Teshome, I. Asselberghs, K. Clays, *Chem. Eur. J.* **2007**, *13*, 7753.
[24] M. J. Crossley, T. W. Hambley, L. G. Mackay, A. C. Try, R. Walton, *J. Chem. Soc. Chem. Commun.* **1995**, 1077.
[25] F. Hof, D. M. Scofield, W. B. Schweizer, F. Diederich, *Angew. Chem.* **2004**, *116*, 5166; *Angew. Chem. Int. Ed.* **2004**, *43*, 5056.
[26] Y. Ishida, H. Ito, D. Mori, K. Saigo, *Tetrahedron Lett.* **2005**, *46*, 109.

[27] T. V. Duncan, K. Song, S.-T. Hung, I. Miloradovic, A. Nayak, A. Persoons, T. Verbiest, M. J. Therien, K. Clays, *Angew. Chem.* **2008**, *120*, 3020; *Angew. Chem. Int. Ed.* **2008**, *47*, 2978.
[28] J. Campo, W. Wenseleers, E. Goovaerts, M. Szablewski, G. H. Cross, *J. Phys. Chem. C* **2008**, *112*, 287.
[29] J. L. Oudar, D. S. Chemla, *J. Chem. Phys.* **1977**, *66*, 2664.
[30] C. H. Wang, *J. Chem. Phys.* **2000**, *112*, 1917; G. Berkovic, G. Meshulam, Z. Kotler, *J. Chem. Phys.* **2000**, *112*, 3997; J. N. Woodford, C. H. Wang, A. E. Asato, R. S. H. Liu, *J. Chem. Phys.* **1999**, *111*, 4621; M. A. Pauley, C. H. Wang, *Chem. Phys. Lett.* **1997**, *280*, 544; P. Kaatz, D. P. Shelton, *J. Chem. Phys.* **1996**, *105*, 3918.
[31] F. Mancois, J.-L. Pozzo, J. Pan, F. Adamietz, V. Rodriguez, L. Ducasse, F. Castet, A. Plaquet, B. Champagne, *Chem. Eur. J.* **2009**, *15*, 2560.
[32] I. C. Pintre, N. Gimeno, J. L. Serrano, M. B. Ros, I. Alonso, C. L. Folcia, J. Ortega, J. Etxebarria, *J. Mater. Chem.* **2007**, *17*, 2219.
[33] Y.-K. Wang, C.-F. Shu, E. M. Breitung, R. J. McMahon, *J. Mater. Chem.* **1999**, *9*, 1449; X. Ma, R. Liang, F. Yang, Z. Zhao, A. Zhang, N. Song, Q. Zhou, J. Zhang, *J. Mater. Chem.* **2008**, *18*, 1756; A. K. Y. Jen, V. P. Rao, K. Y. Wong, K. J. Drost, *J. Chem. Soc. Chem. Commun.* **1993**, 90; S.-S. P. Chou, D.-J. Sun, J.-Y. Huang, P.-K. Yang, H.-C. Lin, *Tetrahedron Lett.* **1996**, *37*, 7279; H. Meier, *Angew. Chem.* **2005**, *117*, 2536; *Angew. Chem. Int. Ed.* **2005**, *44*, 2482; F. Würthner, F. Effenberger, R. Wortmann, P. Kraemer, *Chem. Phys.* **1993**, *173*, 305; R. M. F. Batista, S. P. G. Costa, M. Belsley, M. M. M. Raposo, *Tetrahedron* **2007**, *63*, 9842.
[34] F. Quist, C. M. L. Vande Velde, D. Didier, A. Teshome, I. Asselberghs, K. Clays, S. Sergeyev, *Dyes Pigm.* **2009**, *81*, 203.
[35] G.-D. Peng, A. D. Q. Li, *J. Polym. Sci. Polym. Chem. Ed.* **2001**, *39*, 1794.
[36] G. Olbrechts, R. Strobbe, K. Clays, A. Persoons, *Rev. Sci. Instrum.* **1998**, *69*, 2233.
[37] S. P. Karna, M. Dupuis, *J. Comput. Chem.* **1991**, *12*, 487; H. Sekino, R. J. Bartlett, *J. Chem. Phys.* **1986**, *85*, 976.
[38] J. Tomasi, M. Persico, *Chem. Rev.* **1994**, *94*, 2027; J. Tomasi, B. Mennucci, R. Cammi, *Chem. Rev.* **2005**, *105*, 2999.
[39] H. D. Cohen, C. C. J. Roothaan, *J. Chem. Phys.* **1965**, *43*, S34.
[40] P. J. Davis, P. Rabinowitz in *Numerical Integration*, Blaisdell, London, **1967**, p. 166; for an example of the Romberg Scheme in the case of push–pull π-conjugated systems, see also: B. Champagne, B. Kirtman in *Nonlinear Optical Materials, Vol. 9: Handbook of Advanced Electronic and Photonic Materials and Devices* (Ed.: H. S. Nalwa), Academic Press, San Diego, **2001**, Chapter 2, pp. 63–126.
[41] B. Champagne, B. Kirtman, *J. Chem. Phys.* **2006**, *125*, 024101.
[42] D. Jacquemin, B. Champagne, C. Hattig, *Chem. Phys. Lett.* **2000**, *319*, 327; H. Sekino, R. J. Bartlett, *Chem. Phys. Lett.* **1995**, *234*, 87; J. E. Rice, N. C. Handy, *Int. J. Quantum Chem.* **1992**, *43*, 91.
[43] R. Bersohn, Y.-H. Pao, H. L. Frisch, *J. Chem. Phys.* **1966**, *45*, 3184.
[44] J. Guthmuller, B. Champagne, *J. Chem. Phys.* **2007**, *127*, 164507.
[45] M. Miura, Y. Aoki, B. Champagne, *J. Chem. Phys.* **2007**, *127*, 084103; M. Guillaume, B. Champagne, F. Zutterman, *J. Phys. Chem. A* **2006**, *110*, 13007; Y. Tawada, T. Tsuneda, S. Yanagisawa, T. Yanai, K. Hirao, *J. Chem. Phys.* **2004**, *120*, 8425; D. Rappoport, F. Furche, *J. Am. Chem. Soc.* **2004**, *126*, 1277; A. Masunov, S. Tretiak, *J. Phys. Chem. B* **2004**, *108*, 899; V. Cavillot, B. Champagne, *Chem. Phys. Lett.* **2002**, *354*, 449.
[46] Gaussian 03, Revision D.02, M. J. Frisch, G. W. Trucks, H. B. Schlegel, G. E. Scuseria, M. A. Robb, J. R. Cheeseman, J. A. Montgomery, Jr., T. Vreven, K. N. Kudin, J. C. Burant, J. M. Millam, S. S. Iyengar, J. Tomasi, V. Barone, B. Mennucci, M. Cossi, G. Scalmani, N. Rega, G. A. Petersson, H. Nakatsuji, M. Hada, M. Ehara, K. Toyota, R. Fukuda, J. Hasegawa, M. Ishida, T. Nakajima, Y. Honda, O. Kitao, H. Nakai, M. Klene, X. Li, J. E. Knox, H. P. Hratchian, J. B. Cross, C. Adamo, J. Jaramillo, R. Gomperts, R. E. Stratmann, O. Yazyev, A. J. Austin, R. Cammi, C. Pomelli, J. W. Ochterski, P. Y. Ayala, K. Morokuma, G. A. Voth, P. Salvador, J. J. Dannenberg, V. G. Zakrzewski, S. Dapprich, A. D. Daniels, M. C. Strain, O. Farkas, D. K. Malick, A. D. Rabuck, K. Raghavachari, J. B. Foresman, J. V. Ortiz, Q. Cui, A. G. Baboul, S. Clifford, J. Cioslowski, B. B. Stefanov, G. Liu, A. Liashenko, P. Piskorz, I. Komaromi, R. L. Martin, D. J. Fox, T. Keith, M. A. Al-Laham, C. Y. Peng, A. Nanayakkara, M. Challacombe, P. M. W. Gill, B. Johnson, W. Chen, M. W. Wong, C. Gonzalez, J. A. Pople, Gaussian, Inc., Wallingford, CT, **2004**.

Received: January 26, 2010
Published online: June 8, 2010

